Journal of Machine Engineering, Vol. 9, No. 2, 2009

spindle dynamic properties
machining productivity
machine frame and spindle coupled models
modal Decomposition

Petr KOLAR[1]
Matej SULITKA[1]

COUPLED MODEL OF THE SPINDLE AND MACHINE TOOL FRAME

Influence of the machine frame on the dynamic properties of spindle and tool is investigated using an example of a real machine tool. Model of the whole mechanical system is created as a coupled system of the tool, spindle and machine frame single submodels. Experimental verification of the model has shown a good match of the system critical frequencies and compliances. It has been proved that properties of the machine frame limit the dynamic properties at the tool tip especially in the case, if a compact tool is used.

1. INTRODUCTION

Successful application of high performance machining depends on the chatter-free operation of the whole machine tool. Generally, chatter vibrations result from dynamic properties of the whole machine tool system. Dynamic properties are commonly evaluated by frequency response function (FRF) at the tool centre point (TCP) [1]. This FRF can be significantly influenced only by one part of the system (e.g. a long slim tool or a long ram) or it can be a balanced result of the interaction between the machine tool structure, the spindle and the tool [2]. Moreover, chatter can be influenced also by the feed drive control in specific cases [3].

According to [4] it is suitable to employ the concept of the machine tool virtual modelling for prediction of chatter vibration. Virtual model allows to evaluate the influence of all the machine tool parts, including the tooling system, spindle, machine tool structure and the feed drive control on the chatter vibration origin. Detailed description of the machine tool dynamic properties includes the feed drive control [6] and machine frame structure [e.g. 5].

The aim of this paper is to demonstrate the importance of an appropriate strategy used for modelling the properties of the whole machine tool system. A method for building the

[1] Research Center for Manufacturing Technology, CTU in Prague, Horska 3, 128 00 Prague 2, Czech Republic

coupled model composed of the spindle and machine tool frame is presented and verified by experiments and cutting tests performed on a real machine tool.

2. INFLUENCE OF THE MACHINE TOOL FRAME ON THE DYNAMIC PROPERTIES EVALUATED AT THE SPINDLE AND TOOL

Dynamic properties of the machine tool frame influence the dynamic properties evaluated at the spindle nose. This effect is demonstrated by experiments performed on a three-axis horizontal milling machine. Structure of the machine tool is shown in Fig. 1. The machine tool is equipped with a motorized spindle with maximal speed of 12.000 rpm and maximal power of 25 kW built in the machine ram.

Two different tools have been considered within the testing: milling head with the diameter of 50 mm and length of 60 mm (denoted as H50 – see Fig. 2) and modular shank cutter with the diameter of 32 mm and length of 175 mm (denoted as S32M – see Fig. 3) respectively. The first tool represents an example of a very compact tool used for high performance cutting. The other tool is a typical example of a long compliant tool used for cutting of deep workpieces. Measurements of the FRFs at the spindle nose or the tool tip were performed with the spindle mounted in the machine frame or in the free-free state.

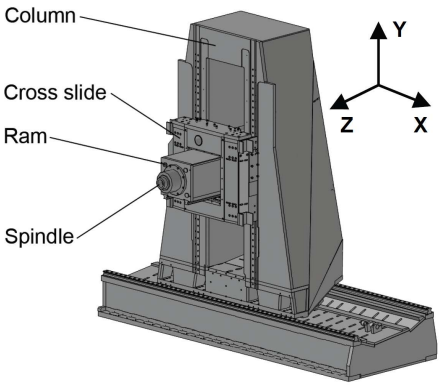

Fig. 1. Machine used for verification

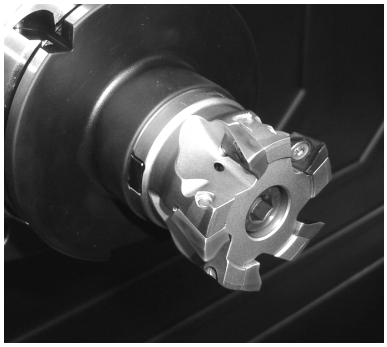

Fig. 2. Milling head H50

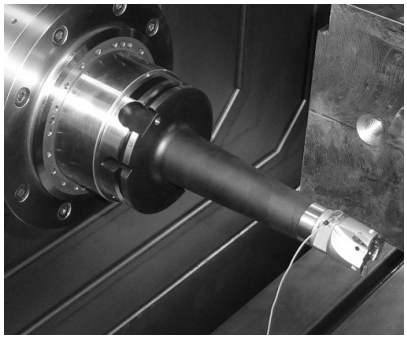

Fig. 3. Shank cutter S32M

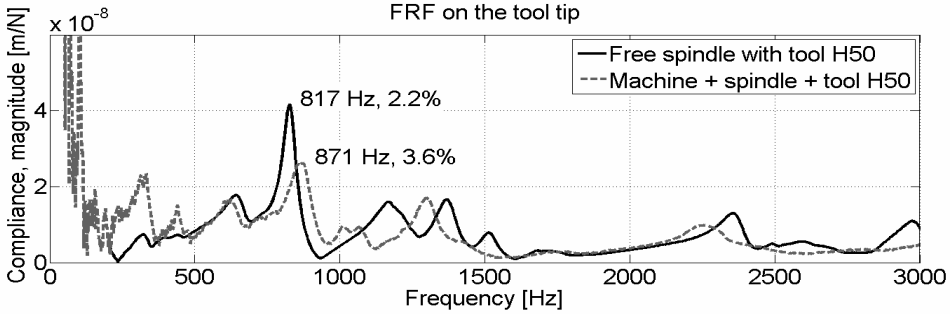

Fig. 4. FRF on the H50 tool tip

Since the H50 tool is light and stiff, the FRF measured in the free-free state is characterized by one significant compliancy close to the frequency of 817 Hz. Other less dominant eigenfrequencies occur in the range of 1000 to 2000 Hz (Fig. 4). If the spindle is mounted in the machine frame, the dominant frequency of the tool-spindle system increases to 871 Hz. Damping of this frequency is also increased. However, the critical compliancy of the whole system is shifted to the low frequency range. This clearly shows that properties of the machine tool frame can be limiting ones if machining with stiff and compact tools is considered.

Fig. 5 shows the FRFs of the spindle with the S32M tool. The tool mounted in the free spindle features one dominant eigenfrequency of 1048 Hz. This frequency remains dominant also if the spindle with the tool is mounted in the machine frame. However, compliancy at this critical frequency is significantly reduced due to the elevated damping of of the spindle and the machine frame system. Despite of this, compliancy related to the discussed eigenfrequency of 1048 Hz is the dominant one and except of the changed level of damping, the machine frame does not exhibit any other influence on the critical dynamic properties of the system.

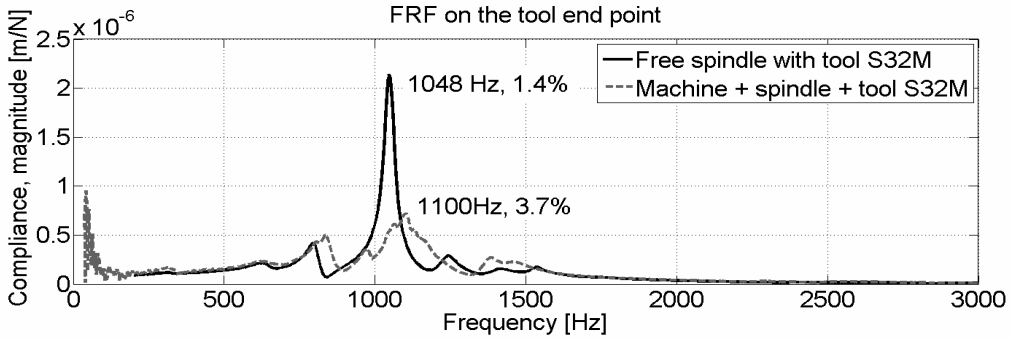

Fig. 5. FRF on the S32M tool tip

As the presented experiments show, the critical compliance of the tool – spindle – machine frame system is influenced by the dynamic properties of each part of this chain. It is therefore important to take into account all of the components of the system when creating the model for evaluation of the FRFs at the spindle nose or the tool tip.

3. MODEL DESCRIPTION

3.1. STRATEGY USED FOR CREATION OF THE COUPLED MODEL OF THE SPINDLE AND MACHINE FRAME SYSTEM

The strategy of coupling the separate FEM models of the spindle and machine frame in modal coordinates is chosen. Each of the models is subject to the modal analysis and transformed into the State-Space description with selection of appropriate number

of eigenfrequencies and interface points. Various approaches to the creation of the machine tool elastic multi-body systems are reported e.g. in [7,8] or [9].

The spindle is connected with the machine ram in two points representing the real fixing of the spindle on its front and back flange. Corresponding pair of interface points is created on the machine frame model as well. The force interaction between the interface points in the spindle front part is established by a translatory spring with high stiffness value in all the three directions. In the spindle back the coupling spring provides rigid connection only in the radial direction.

The machine frame model includes also the representation of the ball screw feed drives. Advanced strategy of the feed drive modelling employs e.g. coupling of the machine frame model with the discrete model of the ball screw feed drive mechanical structure and feed drive control [10]. However, in the frame of the model discussed in this paper, simplified representation of the ball screw feed drive mechanical structure realized by spring elements with high stiffness value of $k = 1.10^{12}$ N/m is considered. This simplification has been assumed with respect to the character of FRF measurements performed with modal hammer, which does not provide the possibility to excite low eigenfrequencies related to the vibration of the ball screw feed drive components.

3.2. SPINDLE MODEL

The spindle model consists of the spindle and tool geometry description, a bearing analytical model and system damping information [11].

The geometry of spindle shaft, spindle housing and tooling system is described by mass and stiffness matrices. The volumetric model of the spindle geometry and its corresponding FE mesh is created in the ANSYS software using the APDL programming language. Guyan's reduction method for reduction of the number of DOFs is applied on the FE mesh with selection of certain nodes. The result is one-dimensional model with elements having 6 DOFs in every node instead of the initial volumetric mesh with 3 DOFs in each node. Properties of the other spindle components (bearings, tool holder-spindle interface) are described by appropriate stiffness matrices.

The bearing stiffness matrix calculation is based on the model described by Jones [12] and Harris [13]. There are three kinds of equations that define the bearing model [14]:

- Hertzian force-deflection characteristics of ball-ring contacts in normal direction;
- force and moment equilibrium on bearing balls;
- geometric formulas stating the relation of bearing ring positions, contact angles and ball-ring normal deflection.

The result of the bearing model is the complete stiffness matrix of each bearing in the assembly with diagonal and off-diagonal terms as well. The model is also able to take into account the thermal state of the spindle [14].

Eigen value problem of an undamped system is solved firstly. In the next step, spindle model is transformed via the modal decomposition technique into the State-Space, in which the modal damping of the system is introduced.

3.3. MACHINE TOOL FRAME MODEL

The computational model of the machine tool structure is based on the simplified geometrical model, which reflects all of the important structural parts of the machine. The geometrical model of the machine tool structure, as well as the computational FE mesh has been prepared in the FEM software I-DEAS. View of the machine FE model with the detailed depiction of one of the interface points for connection with the spindle model can be seen on the Fig. 6. Interface point is connected by rigid constraints (gray solid lines) with a ring of slave nodes.

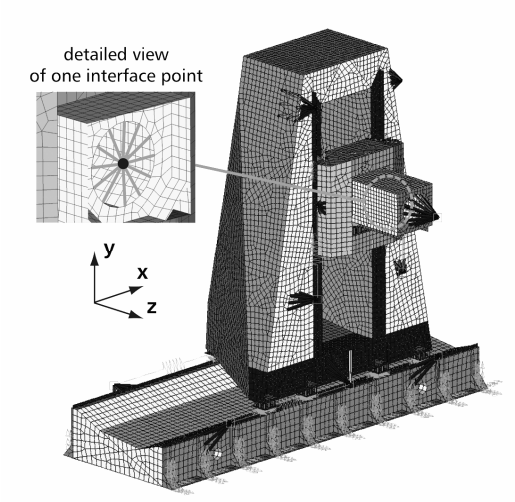

Fig. 6. FEM model of the machine frame

Design of the machine frame features an optimized structure with relatively thin walls and ribs, which allows to represent the machine structure by the shell FE mesh. Quadratic variant of the shell elements is selected.

3.4. CREATION OF THE SPINDLE AND MACHINE FRAME COUPLED MODEL

The coupled model of the spindle and the machine frame system is assembled outside of the FE environment from separate models, which are reduced in modal coordinates. Reduced models are consequently transformed into the State-Space description which keeps the appropriate force inputs and position outputs for establishing the force interactions in physical coordinates.

Linear, time-invariant state space model in modal coordinates is written as

$$\begin{aligned} \dot{\mathbf{q}}_S &= \mathbf{A}\cdot\mathbf{q}_S + \mathbf{B}\cdot\mathbf{u} \\ \mathbf{y} &= \mathbf{C}\cdot\mathbf{q}_S \end{aligned} \tag{1}$$

with $\boldsymbol{u}$ as the input, $\boldsymbol{y}$ output and state vector composed in the modal coordinates as $\mathbf{q}_S = [\dot{\mathbf{q}} \quad \mathbf{q}]^T$. State space matrixes are defined as

$$\mathbf{A} = \begin{bmatrix} \mathbf{0} & \mathbf{E} \\ -\boldsymbol{\Lambda} & -\mathbf{C}_q \end{bmatrix}, \quad \mathbf{B} = \begin{bmatrix} 0 \\ \mathbf{V}^T \end{bmatrix}, \quad \mathbf{C} = [\mathbf{V} \quad \mathbf{0}] \tag{2}$$

where $\boldsymbol{\Lambda}$ is the spectral matrix of eigen-frequencies, $\boldsymbol{C_q}$ diagonal matrix of modal damping and $\boldsymbol{V}$ the modal matrix of eigen-vectors.

Input equation of the State-Space coupled system is obtained by coupling the equations of each of the bodies into one system

$$\begin{bmatrix} {}^1\dot{\mathbf{q}}_S \\ {}^2\dot{\mathbf{q}}_S \end{bmatrix} = \begin{bmatrix} {}^1\mathbf{A} & 0 \\ 0 & {}^2\mathbf{A} \end{bmatrix} \cdot \begin{bmatrix} {}^1\mathbf{q}_S \\ {}^2\mathbf{q}_S \end{bmatrix} + \begin{bmatrix} {}^1\mathbf{B} & 0 \\ 0 & {}^2\mathbf{B} \end{bmatrix} \cdot \begin{bmatrix} {}^1\mathbf{u} \\ {}^2\mathbf{u} \end{bmatrix}, \tag{3}$$

whereby the superscript *1* denotes the body 1 (machine frame) and superscript *2* the body 2 (spindle).

Mutual force interaction between the bodies is defined as

$$-{}^1u_i = {}^2u_i = k_i \cdot ({}^1x_i - {}^2x_i) \tag{4}$$

Expressing the vector of linear displacements $x = \boldsymbol{V}.q$ as a linear combination of shape matrix $\boldsymbol{V}$ and modal coordinates q, after substitution of (4) into (3) the input equation is obtained in the form of

$$\begin{bmatrix} {}^1\dot{\mathbf{q}}_S \\ {}^2\dot{\mathbf{q}}_S \end{bmatrix} = \begin{bmatrix} \mathbf{A}_{C1} & \mathbf{A}_{C2} \\ \mathbf{A}_{C3} & \mathbf{A}_{C4} \end{bmatrix} \cdot \begin{bmatrix} {}^1\mathbf{q}_S \\ {}^2\mathbf{q}_S \end{bmatrix} + \begin{bmatrix} {}^1\mathbf{B}_r & 0 \\ 0 & {}^2\mathbf{B}_r \end{bmatrix} \cdot \begin{bmatrix} {}^1\mathbf{u}_r \\ {}^2\mathbf{u}_r \end{bmatrix}, \tag{5}$$

in which the $\boldsymbol{A}$ matrix is filled with new elements and the $\boldsymbol{B}$ matrix and vector u contain only displacements of nodes r, that are kept as external inputs of the coupled system. In the case of the spindle and machine frame model the system is externally excited on the spindle front.

Output equation of the coupled system is written as

$$\mathbf{y}_C = \mathbf{C} \cdot \begin{bmatrix} {}^1\mathbf{q}_S \\ {}^2\mathbf{q}_S \end{bmatrix} \tag{6}$$

with vector of output coordinates y_C and matrix $\boldsymbol{C}$ defined as

$$\mathbf{C} = \begin{bmatrix} {}^1\mathbf{C}_r & \mathbf{0} & {}^2\mathbf{C}_r & \mathbf{0} \end{bmatrix}, \tag{7}$$

in which the ${}^{\boldsymbol{1}}\boldsymbol{C_r}$ and ${}^{\boldsymbol{2}}\boldsymbol{C_r}$ submatrixes contain the displacements of only the nodes r.

4. VERIFICATION OF THE MODEL

4.1. SPINDLE MODEL VERIFICATION

There is a group of three bearings with TBT arrangement in the front end of the spindle (Fig. 7). The front group uses the FAG HCB 71922 E bearings. The spindle rear end has just one FAG HC 71914 E bearing. The front and the rear bearing group features

constant preload, defined in the model by means of springs. The model of bearing mentioned in chapter 3.2 enable calculation of the bearing stiffness in dependence on shaft revolution (Fig. 8). Influence of thermal field inside of the spindle on bearing stiffness can be neglected because of the dominating effect of spring preload of bearings [10].

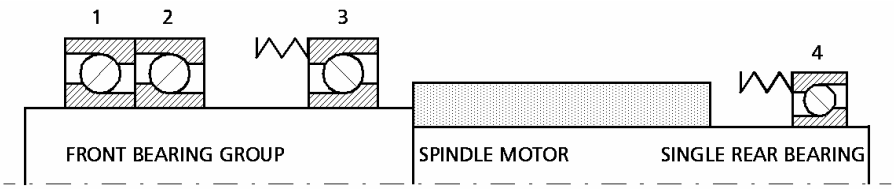

Fig. 7. Scheme of spindle bearings

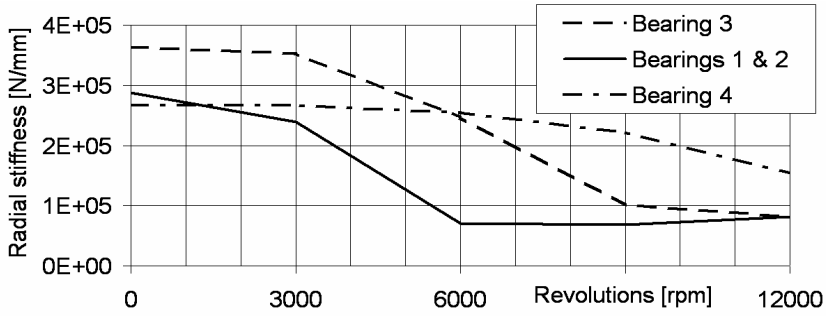

Fig. 8. Bearing stiffness in dependence on revolutions

The spindle was modelled using the method described in chapter 3.2. The mass and stiffness of the shaft is described by FE mesh using quadratic brick elements. The additional masses like motor rotor or draw bar are modelled by beam elements, which connect the nodes selected the FE mesh reduction.

The spindle model has been verified by comparison of the simulated and measured FRFs evaluated at the spindle nose. In the real experiment, the spindle unit was suspended on ropes (Fig. 9). In the computational model, the ropes were represented by additional spring elements connected to the spindle housing. The values of damping for the model were obtained from the measurements.

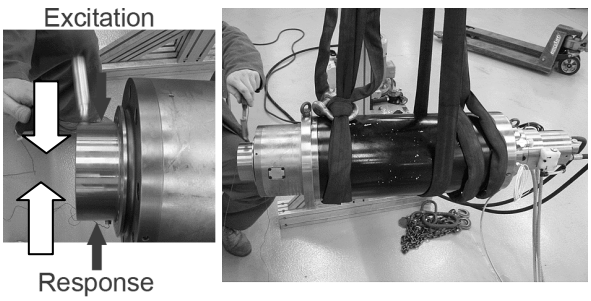

Fig. 9. Measurement of FRF on the hanging spindle

Comparison of the calculated and measured FRFs is given in Fig. 10. Dominant compliancy of the spindle occurs at the eigenfrequency of 856 Hz, whereby very good match of the measured and simulated values of both the critical compliancy and its corresponding frequency can be seen. There are other secondary eigenfrequencies with elevated compliance in the range of 1200 Hz to 2000 Hz. Good correspondence of the computational model with the measurement results is found in the values of compliancy. However, there are some discrepancies in the simulated values of eigenfrequencies. The eigenforms at the frequency of 1281 Hz and 1975 Hz are characterized by bending of the shaft middle section, as illustrated by Fig. 11. In this part of the shaft, the stator of the motor is placed. Stator model could be created only in a simplified form using the beam elements (Fig. 10) due to the missing detailed information on the spindle design and connection between spindle rotor and spindle shaft. Inaccuracy of the simulation model may be attributed to the described simplification of the model.

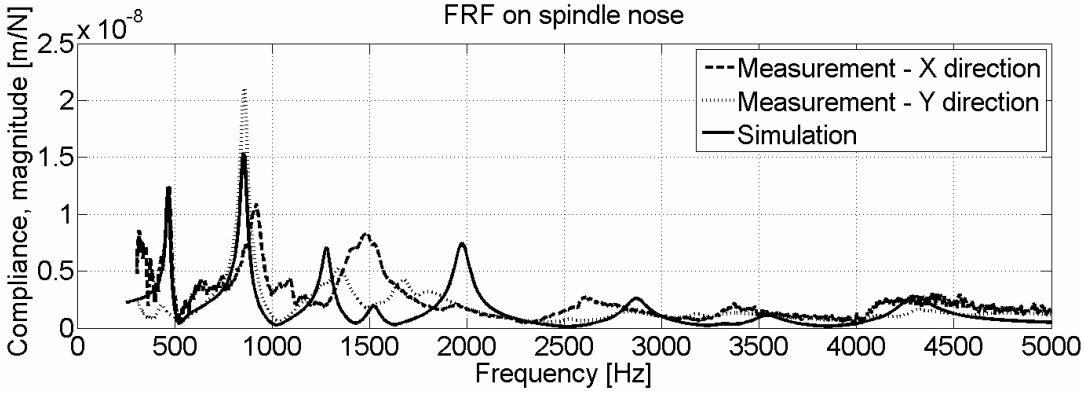

Fig. 10. Comparison of the measured and calculated FRF. of the separate spindle

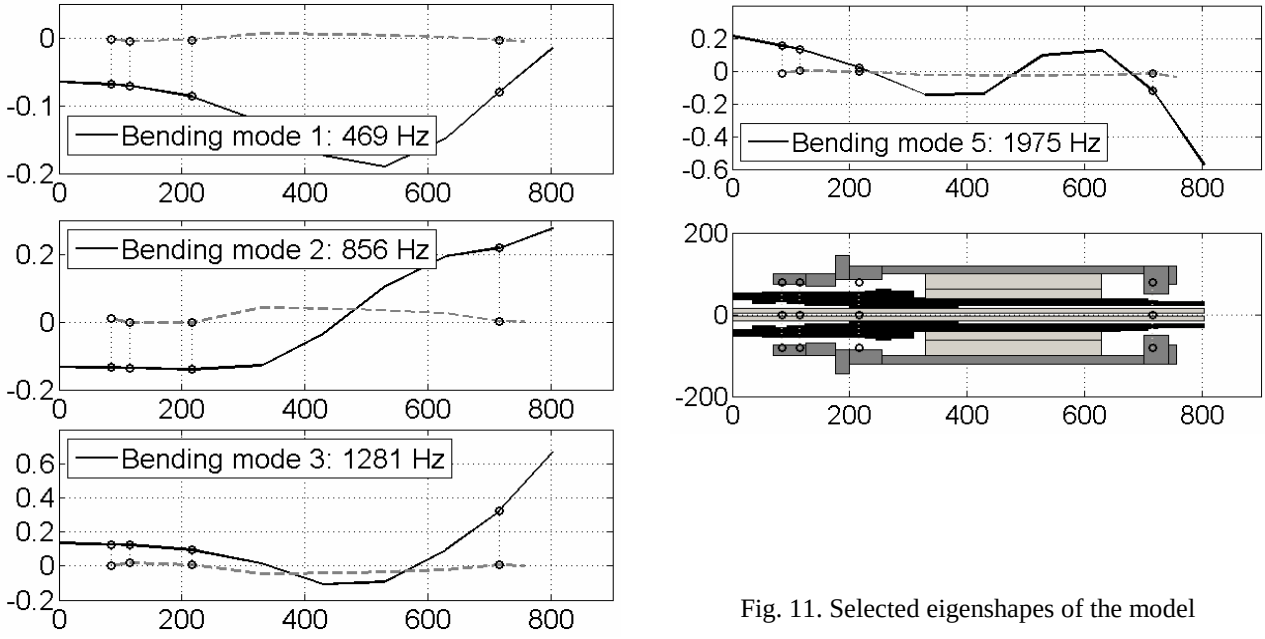

Fig. 11. Selected eigenshapes of the model

4.2. COUPLED MODEL VERIFICATION USING FRF MEASUREMENT

The coupled model includes 50 eigenfrequencies of the machine frame model and all of the eigenfrequencies of the reduced spindle model.

The comparison between the measurement and coupled model in the case of attached milling head H50 can be seen on the Fig. 12. Critical frequencies and their corresponding compliances are in the low frequency range determined by means of the coupled model in a good match with the measurement. It is obvious that these frequencies relate to the vibration of the machine frame. At the computed value of frequency 54 Hz the whole column is deformed in XY plane in a paralelogram-similar shape, at the frequency of 81 Hz free end of the ram is oscillating (Fig. 13). In the higher frequency range, the compliances at the critical frequencies close to 310 Hz and 800 – 900 Hz are well captured by means of the coupled model. The bad match between the measurement and simulation results in frequency range above 1000 Hz is in this case influenced by the simplified modelling of the spindle shaft, as explained in the previous chapter.

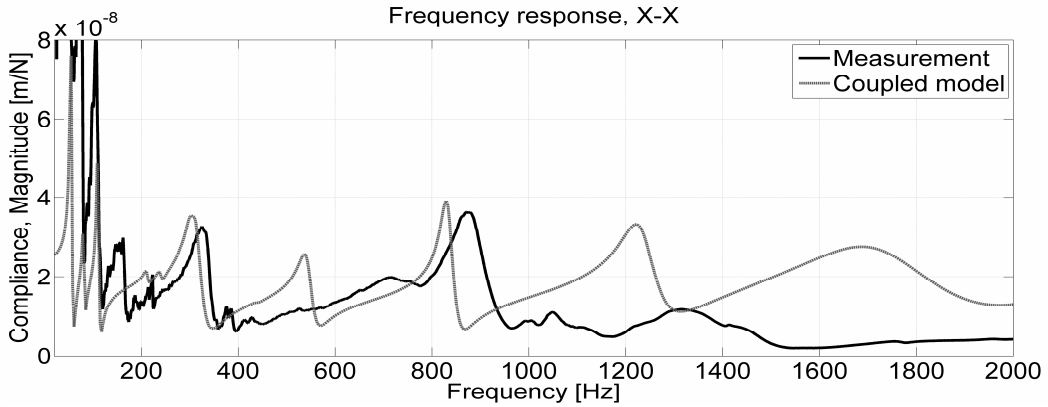

Fig. 12. FRF with the H50 tool

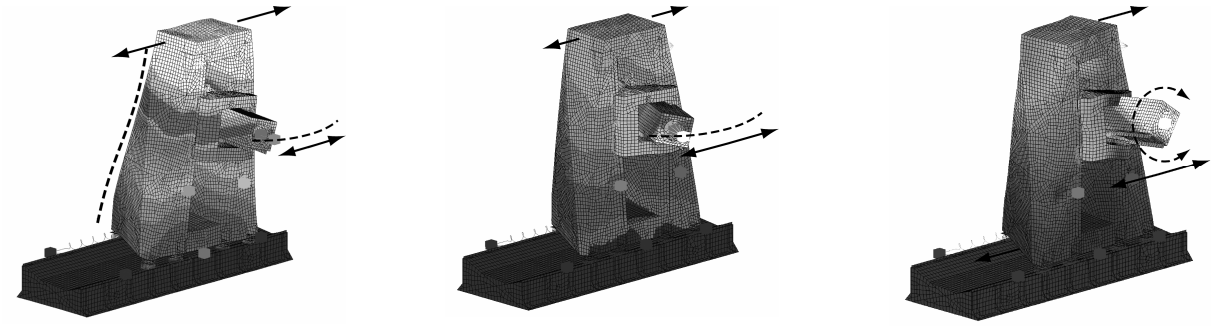

Fig.13. Calculated eigenforms of the machine frame at the frequencies of 54 Hz (left), 81 Hz (middle) and 111 Hz (right)

The above mentioned findings were verified by cutting test of the C45 steel. The steel features the cutting resistance of K_c = 2000 MPa. The milling head H50 was equipped with

inserts Walter ADMT160608R-F56 with coating WSP45. The cutting parameters were: ae = 45 mm, ap = 12 mm, fz = 0.15 mm, n = 1300 and 1600 rpm, vc = 204 and 251 m/min. An accelerometer has been placed at the ram end.

The frequency spectrum of the acceleration signal for two values of the spindle revolutions can be seen in Fig. 14. In both cases the cutting conditions were stable. The dominant amplitude at 107 Hz can be seen in the detail on the bottom left part of the Fig. 14. It is the third eigenfrequency of the machine frame excited by the tooth passing frequency of 108 Hz. There is also another peak at 73 Hz, which relates to the second eigenform of the machine frame. This eigenform was measured at the frequency value of 76 Hz on the machine in static state. This discrepancy could be attributed to the feed drives influence.

The dominant amplitude at 107 Hz can be seen also in the detail on the bottom right part of Fig. 14. The vibration magnitude is smaller because the system is excited by the tooth passing frequency of 133 Hz.

There is also an important vibration magnitude at 533 Hz and at 541 Hz respectively. This is the first spindle frequency which is for the 1600 rpm case higher than the machine structure vibration magnitude at 107 Hz and 133 Hz. It means that the spindle vibrates with the structure. If the tool revolution decreases to 1300 rpm, the spindle vibrations at 541 Hz decrease and the frame vibrations at 73 Hz and 107 Hz increase. It can be seen that the dominant vibration magnitude changes between the structure frequencies and the spindle frequencies depending on the spindle revolutions during the stable cutting.

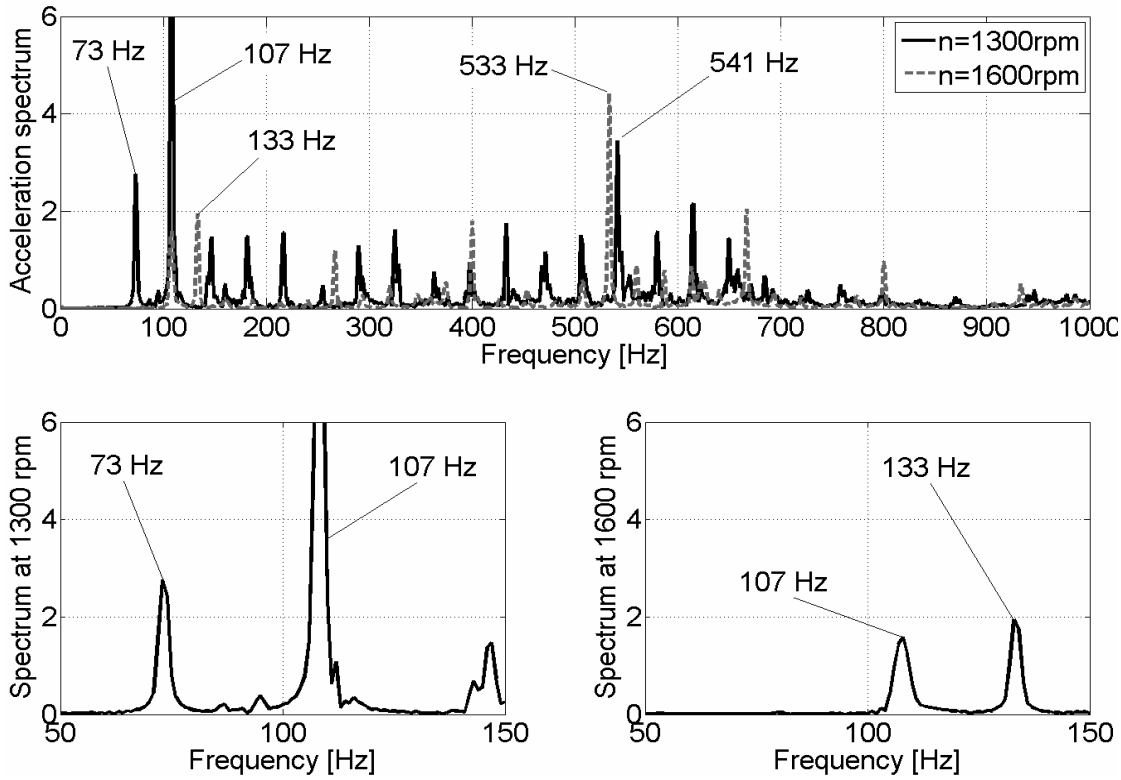

Fig. 14. Acceleration spectrum measured on the ram end. Milling head H50, ae = 45 mm, ap = 12 mm, fz = 0.15 mm

With the thin shank cutter S32M tool, dominant compliancy occurs above the 1000 Hz. The tool is the most compliant part of the system in this case. Between the measured (1180 Hz) and simulated (1060 Hz) value there is the difference of about 11 % (Fig. 15). This dominant compliancy can be found also in the spectrum of vibration signal measured during the cutting test of the C45 steel. The tool S32M was equipped with inserts Walter ADMT160608R-F56 with coating WSP45 again. The cutting parameters were: ae = 32 mm, ap = 3 mm, fz = 0.12 mm, n = 2100 rpm, vc = 211 m/min. The spectrum of acceleration signal is shown in Fig. 16.

The cutting conditions caused unstable cut. The tool eigenfrequency at 1173 Hz can be seen in the detail on the bottom part of Fig. 16. There are also other peaks resulting from the unstable cut. The peaks have distance of 35 Hz which is the revolution frequency [1].

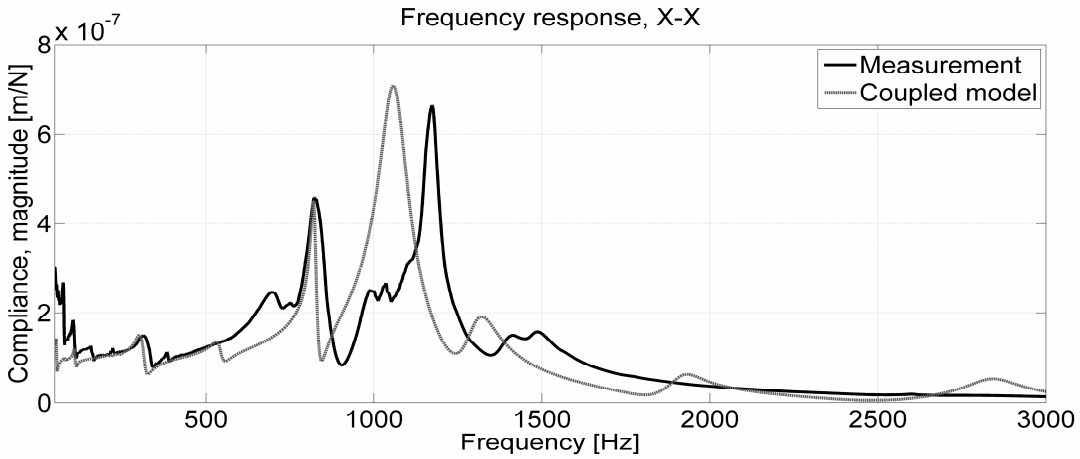

Fig. 15. FRF with the S32M tool

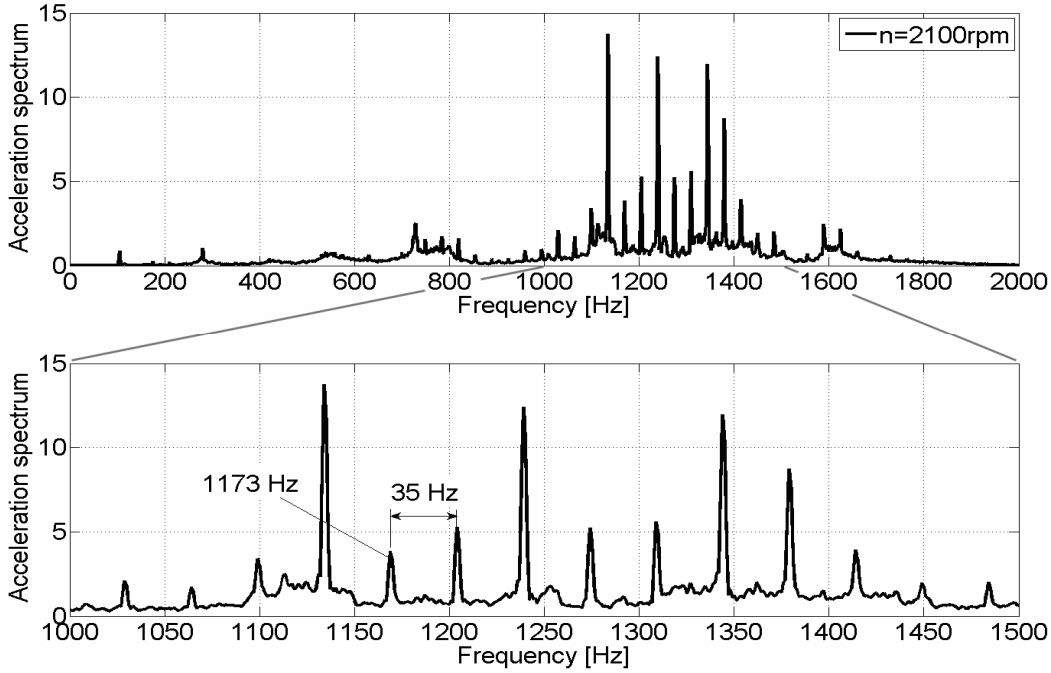

Fig. 16. Acceleration spectrum measured on the ram end. Shank cutter S32M, ae = 32 mm, ap = 3 mm, fz = 0.12 mm

5. CONCLUSION

The model which couples the properties of a spindle and a machine tool frame has been presented. The properties of the whole machine tool system have been evaluated at the tool tip. The model has been verified experimentally with a good match between measured and simulated critical frequencies and compliances. Ball screw feed drives have been modelled in the machine frame model by means of a simplified representation of springs with high stiffness value.

Results reveal that it is important to take into account also the dynamic properties of the machine frame mainly for roughing operations with compact cutting head. A machine frame is characterized by low eigenfrequencies, typically of up to 200 Hz, which may show significantly higher compliance than those related to the spindle – tool system. Structural eigenforms at low frequencies may be excited by cutting process (especially aggressive roughing) and machine tool performance may be limited in this way.

On the contrary, machining with thin tools is usually not affected by the properties of the machine tool frame since a single frequency resulting from tool's bending is critical. The whole machine structure shows its influence only indirectly through the changed level of structural damping.

Determination of critical compliances and frequencies of the spindle and machine frame coupled system will be investigated by other experimental approaches, which will use e.g. excitation of the machine structure by means of feed drives. Procedure of the spindle and machine frame coupled model creation will be verified using other examples of machine tools. Issue of the feed drive control influence on the dynamic properties evaluated at the tool tip will be investigated by extension of the coupled model by the feed drive complex model.

ACKNOWLEDGEMENT

This research has been supported by the 1M0507 grant of the Ministry of Education, Youth and Sport of the Czech Republic.

REFERENCES

[1] ALTINTAS Y., WECK M., 2004, *Chatter stability of metal cutting and grinding*. Annals of CIRP 53/2/619–642.

[2] CAO Y., ALTINTAS Y., 2007, *Modeling of spindle-bearing and machine tool systems for virtual simulation of milling operations*. International Journal of Machine Tools and Manufacture, 47/9/1342-1350.

[3] SOUCEK P., 2008, *Feed drive influence on machining process stability*. International Congress MATAR PRAHA - Proceedings of Part 2: Testing, Technology. Prague, Society for machine tools, 75-80. ISBN 978-80-904077-0-1.

[4] ALTINTAS Y., BRECHER C., WECK M., WITT S., 2005, *Virtual Machine Tool*. Annals of CIRP 54/ 2/115-138.

[5] SMOLIK J., 2008, *Primary structural parts of machine tools made from unconventional materials*. International Congress MATAR PRAHA 2008 - Proceedings of Part 1: Drives & Control, Design, Models & Simulation. Prague, Society for machine tools, 65-70. ISBN 978-80-903421-9-4.

[6] ZAEH M. F., HENNAUER M., POEHLER A., 2007, *The Machine Tool of Tomorrow: An Optimised, Complete System*. 6th International Conference on High Speed Machining, 21-22.
[7] MAJ R., BIANCHI G., 2005, *Mechatronic analysis of machine tools*. 9th SAMTECH Users Conference 2-3 February Paris, France.
[8] HOFFMANN F., BRECHER C., 2005, *Simulation von Verfahroperationen*. Werkstattstechnik online, Jahrgang 95 H. 7/8/506-12.
[9] LEHNER M., EBERHARD P., 2006, *Modelreduktion in elastischen Mehrkörpersystemen*. Automatisierungstechnik, Jahrgang 54 H. 4/170-177.
[10] VESELY J., SULITKA M., 2008, *Machine Tool Virtual Model*. International Congress MATAR PRAHA. Proceedings of Part 1: Drives & Control, Design, Models & Simulation. Prague, Society for machine tools, 115 - 122. ISBN 978-80-903421-9-4.
[11] KOLAR P., HOLKUP T., 2007, *Modeling of a Machine Tools Spindle using a Hybrid Model*. Proceedings of 3rd International Conference - Virtual Design and Automation. CD-ROM, paper No. S05_06_01_kolar. 8p
[12] JONES A.B., 1960, *A general theory for elastically constrained ball and radial roller bearings under arbitrary load and speed conditions*. Journal of Basic Design, Transactions of the ASME, 309-320.
[13] HARRIS T.A.: Rolling Bearings Analysis. Third Edition. New York: John Wiley & Sons 1991.
[14] HOLKUP T., HOLY S., 2006, *Complex modelling of spindle rolling bearings*. Journal of Machine Engineering - Eficiency Development of Manufacturing Machines, 6/3/48-61. ISSN 1895-7595.